Article

The effect of molybdenum on precipitation behaviour in austenitic strip-cast steels containing niobium

Lu Jiang[1*], Ross K.W. Marceau[1], Thomas Dorin[1], Huaying Yin[1], Xinjun Sun[2], Peter D. Hodgson[1], Nicole Stanford[3]

[1] Deakin University, Institute for Frontier Materials, Geelong, VIC 3216, Australia
[2] Department of Structural Steels, Central Iron and Steel Research Institute, Beijing, 10008, China
[3] Future Industries Institute, University of South Australia, Mawson Lakes, SA 5095, Australia
* Correspondence: l.jiang@deakin.edu.au

Abstract: Two low-C steels microalloyed with Nb were fabricated by simulated strip casting, one with Mo and the other without Mo. Both alloys were coiled at 900 °C to investigate the effect of Mo on the precipitation behaviour in austenite in low-C strip-cast Nb steels. The mechanical properties results show that during the coiling at 900 °C the hardness of both alloys increases and reaches a peak after 3000 s and then decreased after 10,000 s. Additionally, the hardness of the Mo-containing alloy is higher than that of the Mo-free alloy in all coiling conditions. Thermo-Calc predictions suggest that MC-type carbides exist in equilibrium at 900 °C, which are confirmed by transmission electron microscopy (TEM). TEM examination shows that precipitates are formed after 1000 s of coiling in both alloys and the size of the particles is refined by the addition of Mo. Energy dispersive spectroscopy (EDS) and electron energy loss spectroscopy (EELS) reveal that the carbides are enriched in Nb and N. The presence of Mo is also observed in the particles in the Nb-Mo steel during coiling. The concentration of Mo in the precipitates decreases with increasing particle size and coiling time. The precipitates in the Nb-Mo steel provide significant strengthening increments of up to 140 MPa, much higher than that in the Nb steel, ~ 96 MPa. A thermodynamic rationale is given, which explains that the enrichment of Mo in the precipitates reduces the interfacial energy between precipitates and matrix. This is likely to lower the energy barrier for their nucleation and also reduce the coarsening rate, thus leading to finer precipitates during coiling at 900 °C.

Keywords: Molybdenum; Precipitation; Austenite; Niobium Steels; Strip Casting

1. Introduction

For the high-strength low-alloy (HSLA) steels containing niobium (Nb) produced by conventional casting techquies, hot deformation in the austenite region usually induces the formation of Nb carbonitrides precipitates [1, 2]. The Nb carbonitrides, formed in austenite, are able to provide precipitation strengthening and refine the microstructure by delaying the recrystallization of austenite at high temperatures, improving the strength as a result [2, 3]. However, these precipitates can be eventually very coarse after a prolonged isothermal-holding in the austenite region, consequently losing their advantage in the microstructure refinement and precipitation strengthening. In previous literature, trace additions of molybdenum (Mo) were reported to enhance the precipitation strengthening of steels microalloyed with Nb or/and Ti by suppressing the coarsening of Nb or Ti carbides [4-10]. It was proposed that Mo changes the coarsening resistance of Nb-rich carbonitrides in austenite by lowering interfacial energy [11], and thus refines the precipitates [11, 12]. However, despite the extensive investigations on the effect of Mo on the formation of Nb-rich precipitates in austenite, the mechanisms behind these observations are not well established.

Unlike conventional steel-making processes that usually undergo several controlled hot-rolling passes, direct strip casting (DSC) combines casting and subsequent hot-rolling into a single and continuous

Preprints (www.preprints.org) | NOT PEER-REVIEWED | Posted: 6 September 2020 doi:10.20944/preprints202009.0150.v1

route with extremely rapid solidification and high cooling rates [1-3], which reduces cost and saves energy-consumption up to 90%. Dorin et al. [13] studied the formation of Nb(C, N) in strip-cast steels and found that chemically complex Nb-rich precipitates containing C, N, Si and S were formed in austenite during coiling at a high temperature (850 °C), which provides a significant strength increment of up to ~ 150 MPa. This early work also emphasized significant differences in the Nb(C, N) precipitates formed in strip-cast materials as compared to the ones formed in conventionally processed steel. One of the main differences is that strip casting produces as-cast samples where the Nb is supersaturated and the precipitates can then be formed during a controlled coiling treatment [14]. Consequently, precipitation occurs in non-deformed austenite. Thus, the mechanism behind the precipitation can be different to the strain-induced precipitation in previous literature. To the best of our knowledge, the effect of Mo on the precipitation of Nb(C, N) in the austenite phase field of strip-cast steels has rarely been studied.

In the present paper, two Nb-containing low-carbon steels were prepared via strip casting with and without Mo. The as-cast samples were then coiled at 900 °C for different durations and hardness testing was used to monitor the hardening response during coiling. Transmission electron microscopy (TEM) was performed to observe the precipitation for different coiling times. Finally, the thermodynamic effects of Mo on Nb-rich precipitates and corresponding precipitation strengthening are also presented.

2. Materials and Methods

The compositions of the alloys studied in this work are listed in Table 1. The steels were cast using a lab-scale strip casting simulator, known as a dip tester [15]. The steels were melted in a 75 kW induction furnace using high purity starting elements. The details of the casting process can be found in [16, 17]. After casting, the samples were immediately transferred into a preheated muffle furnace within 2 s, and within this time the samples did not cool below the coiling temperature of 900 °C. The detailed thermal profile and schedule diagram of coiling treatment can be found in [16]. Coiling times varied from 100 to 10,000 s, and all samples were air-cooled to room temperature at the end of the coiling treatment.

Table 1. Compositions of the studied alloys, wt.%.

	C	Mn	Si	Al	Nb	Mo	S	N	Fe
Nb steel	0.05	1.45	0.21	0.003	0.05	-	<0.0005	0.01	bal.
Nb-Mo steel	0.05	1.50	0.23	0.004	0.05	0.33	<0.0005	0.01	bal.

Thermo-Calc software with TCFE 9: Steels/Fe Alloys v9.0 database was used to check to the equlibrium phases at 900 ºC for the two steels, as displayed in Fig. 1. It can be seen that at 900 °C MC-type carbides can be formed in the austenite region and the theoretical volume fraction of these carbides in equilibrium is ~ 0.0605%.

Preprints (www.preprints.org) | NOT PEER-REVIEWED | Posted: 6 September 2020 doi:10.20944/preprints202009.0150.v1

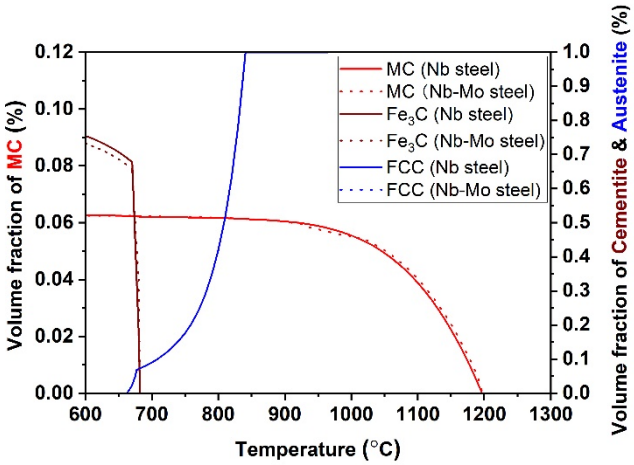

Figure 1 Volume fractions of MC, austenite and cementite in equilibrium, as predicted by Thermo-Calc software with TCFE 9: Steels/Fe Alloys v9.0 database.

Hardness tests were carried out at room temperature to monitor the hardness evolution of both steels coiled at 900 °C for various times. Average values were generated from at least 7 measurements for each condition.

Samples examined by optical microscopy were prepared by sectioning parallel to the casting direction. The specimens were ground using increasingly finer grades of silicon carbide paper, followed by polishing using diamond particles solutions. Polished samples were etched in 4% nital solution for 10 s. Optical micrographs were taken using Olympus HR DP70 microscope.

TEM foils were electropolished in a solution of 5% perchloric acid in methanol using a twin-jet Tenupol unit, running at 30 V and ~ -35 °C. Carbon layers for TEM carbon replica samples were prepared using a JEOL JEE-420 Vacuum Evaporator and supported by 300 square mesh copper grids. TEM observation was performed on Philips CM20 instrument with a LaB_6 filament operating at 200 kV. Composition analysis of precipitate particles was carried out using JEOL FEG 2100F TEM with JED-2300T energy dispersive spectroscopy (EDS) detector, operating at 200 kV. Gatan GIF Quantum 965 post column electron energy loss spectroscopy (EELS) analysis was carried out for fine composition examination using an energy range of 0 to 1000 eV.

3. Results

3.1 Hardness

Hardness measurements were conducted on the two steels for different durations of coiling at 900 °C, as shown in Figure 2. The as-cast hardness of both the Nb and Nb-Mo steels was ~ 201 HV indicating the minor effect of 0.33 wt.% Mo to the Nb steels in the as-cast condition. This has been explained by the very small solid solution strengthening from the addition of Mo in solid solution when the as-cast microstructure of both alloys is very similar [18]. As coiling treatment progresses, the hardness of both alloys evolves in a similar manner. In the early stage (before 100 s), the hardness slowly increases. Afterwards, a more rapid hardening occurs in both alloys by reaching the peak hardness after 3000 s at 900 °C. The Nb-steel and Nb-Mo-steel reached peak hardness values of 225 and 245 HV, respectively. However, after 10,000 s coiling the hardness of both steels drops. Generally, the hardness of the Nb-Mo steel is higher than that of the Nb steel.

Preprints (www.preprints.org) | NOT PEER-REVIEWED | Posted: 6 September 2020 doi:10.20944/preprints202009.0150.v1

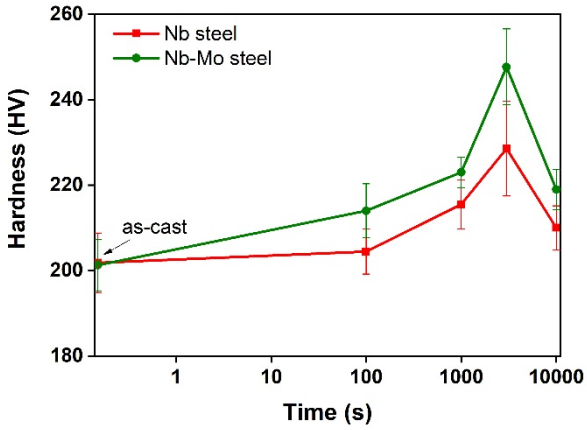

Figure 2 Hardness evolution of the Nb and Nb-Mo steels during coiling at 900 °C.

3.2 Microstructure

The microstructure of the two steels coiled at 900 °C for 100 and 10,000 s were examined and shown in Fig. 3. Both microstructures are mainly bainitic, similar to the as-cast microstructure [16], however some grain boundary allotriomorphic ferrite formed in the Nb steel after 10,000 s coiling at 900 °C, but not in the Nb-Mo steel. The formation of allotriomorph ferrite in strip-cast Nb-steel was already reported in an earlier study [13]. The allotriomorphic ferrite forms during the isothermal treatment at 900 °C, the bainite then forms upon cooling from the coiling temperature. For the case of the Nb-Mo steel, the suppression of the ferrite formation during coiling is due to the solute drag by Mo, which has been discussed in [16].

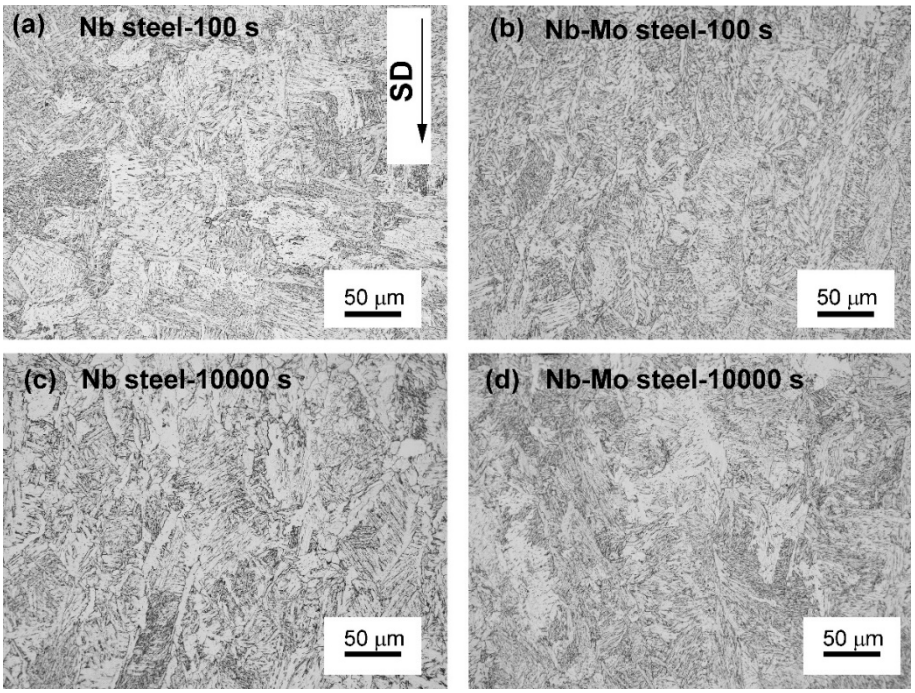

Figure 3 Optical images of the microstructure of the Nb (a & c) and Nb-Mo (b & d) steels coiled for 100 and 10,000 s at 900 °C. (Solidification direction (SD) is shown by the arrow.)

3.3 TEM

Bright-field (BF) TEM images of carbon replicas produced from the Nb and Nb-Mo steels coiled at 900 °C for various times are shown in Fig. 4. Precipitation does not occur after coiling for 100 s and only

Preprints (www.preprints.org) | NOT PEER-REVIEWED | Posted: 6 September 2020 doi:10.20944/preprints202009.0150.v1

some coarse spherical particles around 250 nm in diameter are observed in both steels (Fig. 4 a & e). After 1000 s of coiling at 900 °C, precipitates are formed on grain boundaries and dislocations. From the Thermo-Calc calculation in Fig. 1, these precipitates are MC-type carbides. The size of the carbides in both steels increases as a function of coiling time, Fig. 5. Generally, the particle size in the steel containing Mo is smaller than that in the Mo-free steel.

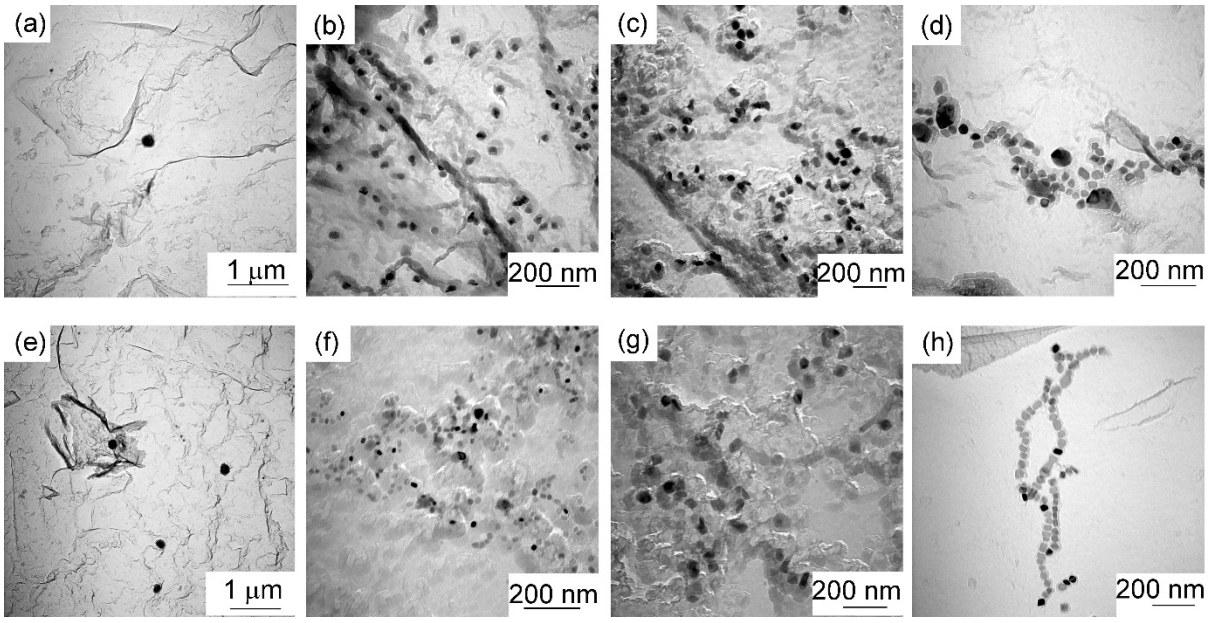

Figure 4 Bright-field (BF) TEM images of the carbon replicas of the Nb (a – d) and Nb-Mo (e – f) steels coiled at 900 °C for 100 s, 1000 s, 3000 s and 10,000 s, from left to right. Note scale bar changes.

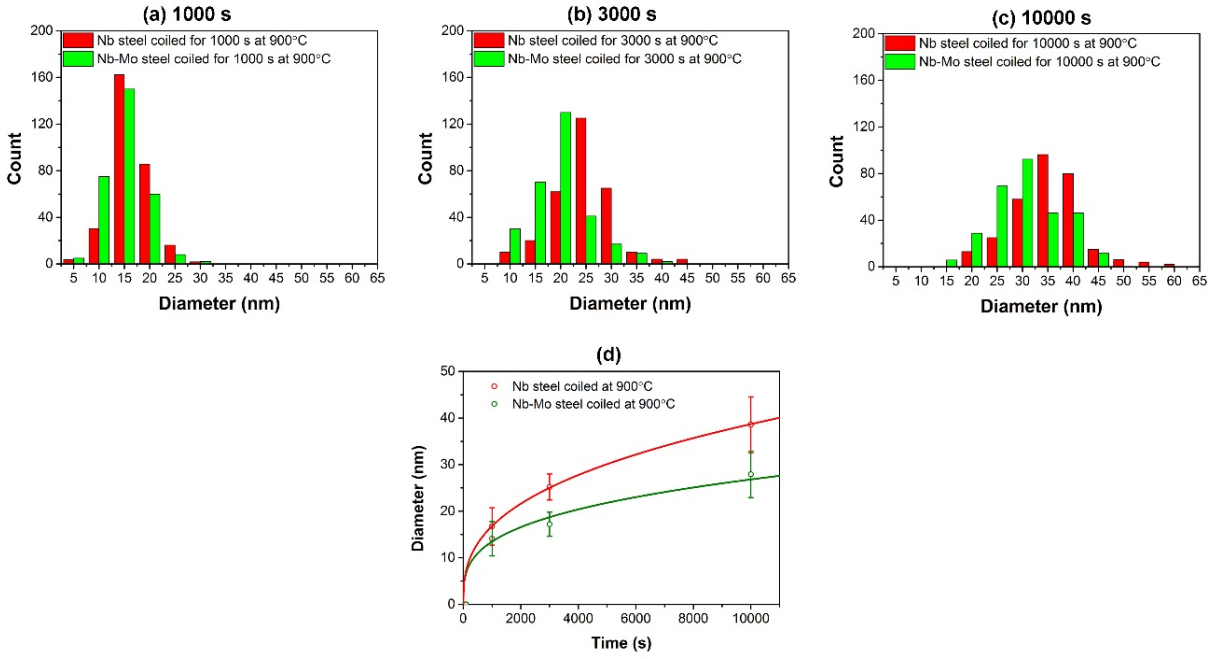

Figure 5 Size distributions (a – c) of the carbides in the Nb and Nb-Mo steels coiled at 900 °C for 1000 s, 3000 s and 10,000 s, respectively. (d) is the average particle size evolution of the two steels during coiling at 900 °C.

The compositions of carbides formed in both alloys coiled at 900 °C for 10,000 s were analysed by TEM-EDX, as shown in Fig. 6. The carbides in both steels are enriched in Nb, S and N. In the Nb-Mo steel,

Preprints (www.preprints.org) | NOT PEER-REVIEWED | Posted: 6 September 2020 doi:10.20944/preprints202009.0150.v1

the carbides also contain Mo. However, Nb (L), Mo (L) and S (K) peaks overlap in EDX spectrum, which presents difficulty for accurate compositional analysis of the carbides. Therefore, EELS was utilised to confirm the presence of Nb, Mo and S in the carbides, as shown in Fig. 7. The carbides in the Nb-Mo steel coiled at 900 °C are clearly enriched in Nb and Mo. However, whilst S is not identified to be present in all the precipitates, minor S segregation was observed at some precipitates. This result agrees with earlier reports of the presence of S in the Nb-carbonitrides formed in austenite [13].

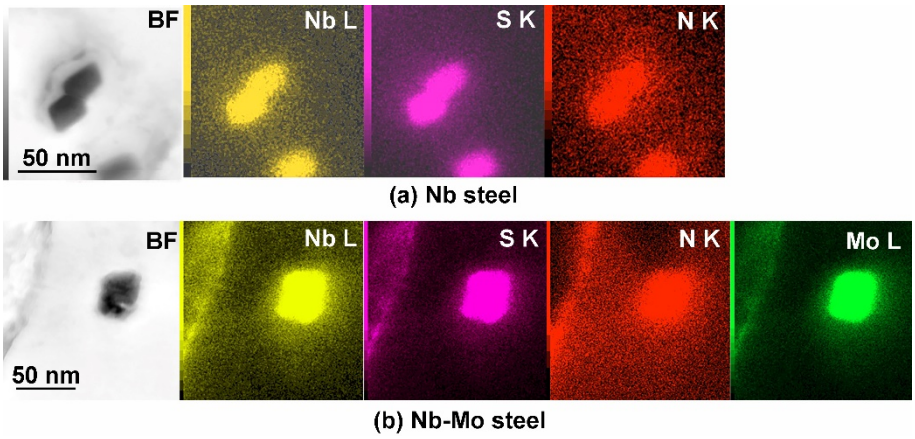

Figure 6 Bright-field (BF) TEM image and corresponding EDX chemical maps for the carbon replicas of precipitates in the (a) Nb and (b) Nb-Mo steels coiled at 900 °C for 10,000 s.

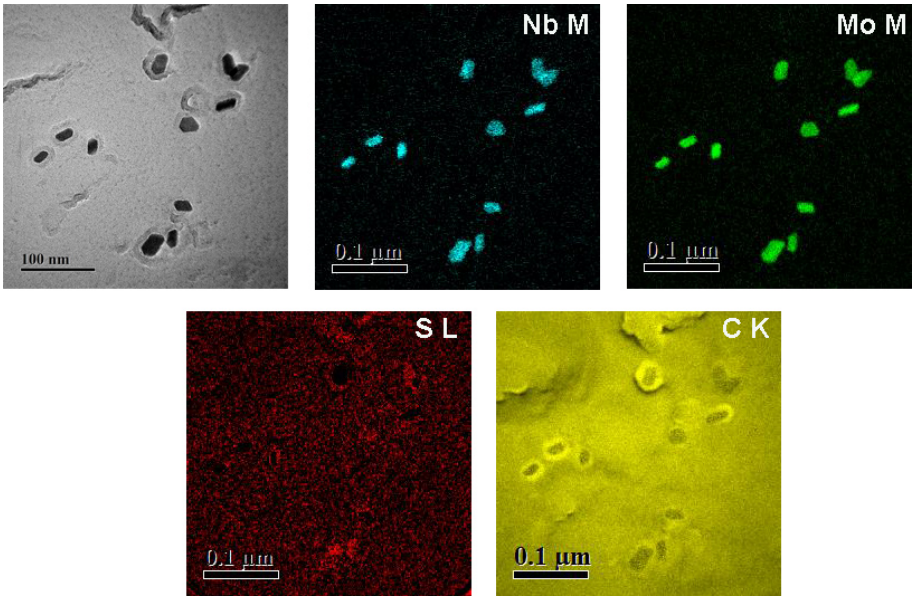

Figure 7 EELS examination for the chemistry of the precipitates in the Nb-Mo steel coiled at 900 °C for 3000 s.

Based on TEM-EDX analysis, the Mo/(Nb + Mo) composition ratio of the carbides in the Nb-Mo steel coiled at 900 °C are presented in Fig. 8. It can be seen that the ratio significantly decreases with increasing coiling time and particle size. This suggests that Mo atoms play an important role during the nucleation at the early stages of the precipitation kinetics at 900 °C. As the precipitates coarsen, however, the they are mainly enriched in Nb given the decrease in the Mo/(Nb + Mo) ratio as a function of coiling time. This growth mechanism can be rationalized by the difference in diffusivities between Nb and Mo [19-21].

Preprints (www.preprints.org) | NOT PEER-REVIEWED | Posted: 6 September 2020 doi:10.20944/preprints202009.0150.v1

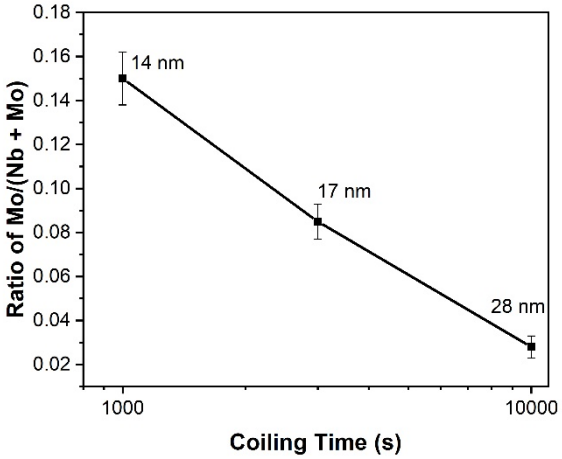

Figure 8 Mo/(Nb + Mo) ratio of carbides formed in the Nb-Mo steel coiled at 900 °C for various times.

4. Discussion

4.1 The effect of Mo on the thermodynamics of precipitation

In the austenite region, the solid solubility products of NbC, NbN and MoC are obtained from [12, 22]:

$$\log[\mathrm{Nb}]\cdot[\mathrm{C}] = 5.43 - 10960/T \quad (1)$$

$$\log[\mathrm{Nb}]\cdot[\mathrm{N}] = 6.163 - 7583/T \quad (2)$$

$$\log[\mathrm{Mo}]\cdot[\mathrm{C}] = 4.96 - 12230/T \quad (3)$$

where, $[M]$ is the weight percentage of element M in solid solution. As $(\mathrm{Nb},\mathrm{Mo})(\mathrm{C},\mathrm{N})$ carbonitride can be treated as a solution that is composed of NbC, NbN and MoC and having NaCl-type structure, the $(\mathrm{Nb_{k1+m1}},\mathrm{Mo_{k2}})(\mathrm{C_{k1+k2}},\mathrm{N_{m1}})$ formula was used in the present work for the thermodynamic and kinetic discussion. Here, $k1, k2$ and $m1$ are the mole fractions for NbC, MoC and NbN and $k1 + k2 + m1 = 1$. Through calculation, the equilibrium ratio of Mo/(Nb+Mo) at 900 °C is 0.00177, which indicates that the precipitates observed in this work were thermodynamically unstable and did not have an equilibrium composition, as shown in Fig. 8.

It is well-known that microalloyed carbonitrides formed in the austenite matrix typically keep a cube-on-cube orientation relationship with the matrix [22]. Therefore, the lattice misfit can be calculated as:

$$\delta = \left|\frac{a_{M(C,N)} - a_\gamma}{a_{M(C,N)}}\right| \quad (4)$$

where, $a_{M(C,N)}$ and a_γ are the lattice parameters for carbonitrides $\mathrm{M(C,N)}$ and austenite, respectively. From the literature [22, 23], the austenite lattice parameter is taken here to be 0.36615 nm, and the lattice parameter for $(\mathrm{Nb_{k1+m1}Mo_{k2}})(\mathrm{C_{k1+k2}},\mathrm{N_{m1}})$ can be obtained by using the linear interpolation method [12]. The interfacial energy can be calculated as:

$$\alpha = \frac{E a_\alpha}{4\pi(1-\nu^2)} f(\delta) \quad (5)$$

where E is the elastic modulus (208.2 GPa [23]), ν is the Possion's ratio (0.32 [24]) and

$$f(\delta) = \delta\left[\frac{2}{1+\frac{1}{4\delta^2}} - \ln(2\delta)\right] \quad (6)$$

Figure 9 shows the interfacial energy between the precipitates and the austenite matrix as a function of temperature. It can be seen that the precipitates in the Nb-Mo steel have a lower interfacial energy than

Preprints (www.preprints.org) | NOT PEER-REVIEWED | Posted: 6 September 2020 doi:10.20944/preprints202009.0150.v1

in the Nb steel when coiled at 900 °C. This is contrary to previous work that reported an increase in Gibbs free energy when adding Mo to MC precipitates [7, 25]. According to the classic theory of nucleation [22, 23, 26], the increase of Gibbs free energy (absolute value) reduces the driving force for precipitation, while the decrease of interfacial energy is beneficial for precipitation. Thus, there is a competition between the effect that Mo has on the Gibbs free energy and on the interfacial energy. The decrease in interfacial energy from Mo is responsible for the enhanced nucleation of the carbonitrides. This explains the high concentration of Mo in the precipitates at the early stages of precipitation and also the smaller size of the precipitates in the Mo-containing steel.

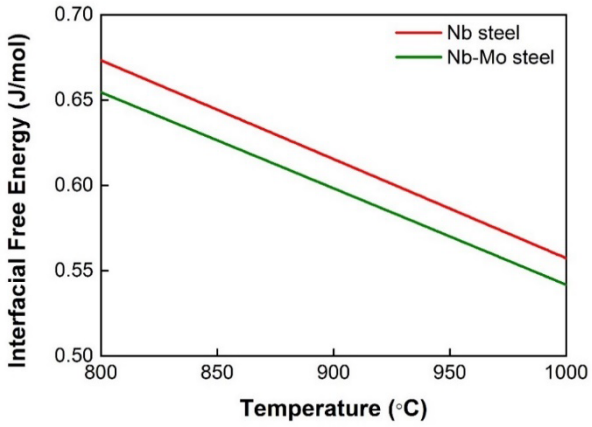

Figure 9 Interfacial free energy of the precipitates formed in austenite for the two steels.

4.2 The effect of Mo on the coarsening kinetics of precipitation

The influence of Mo in the Ostwald ripening stage of precipitation was quantified using LSW theory [27, 28], which predicts the average size of particles when the volume fraction of precipitation is small:

$$\overline{r_t} = \overline{r_0}(1 + k\sigma D c_0 t)^{1/3} \quad (6)$$

where $\overline{r_t}$ and $\overline{r_0}$ are the average particle radius and nucleus radius, respectively. D and c_0 are the diffusivity and mole concertation of the controlling element respectively, t is the coiling time, and k is a constant parameter. The controlling element can be determined by the value of the product $D{\cdot}c_0$. At 900 °C, $D{\cdot}c_{0\text{-}Nb}$ ($= 9.9 \times 10^{-17}$) is smaller than $D{\cdot}c_{0\text{-}Mo}$ ($= 4.3 \times 10^{-16}$) [21]. Thus, Nb is the rate-limiting element in both steels. Therefore, the coarsening of the precipitates in both alloys when coiling at 900 ºC is dependent on the interfacial energy σ, which was lower in the Nb-Mo steel than in the Nb steel. Consequently, the coarsening rate of precipitates in the Nb-Mo steel coiled at 900 °C is smaller than that in the Nb steel, leading to a smaller particle size (Fig. 5). Additionally, as mentioned above, the diffusion of Mo between precipitates and matrix also slows the growth and coarsening of particles.

4.3 Precipitation hardening

A simple yield strength model was used to better understand the strengthening contribution from the precipitates. As shown in Figure 3, the bulk microstructure of both steels is very similar and mainly consists of bainite. For simplicity, we consider that the strength increment observed during coiling comes mainly from the precipitates. The equivalent yield strength is obtained by converting the hardness values as per the equation ($\sigma_y = 3.06H_v$) in [29]. After coiling for 100 s at 900 °C, the strength of the Nb-Mo steel increases by ~ 25 MPa, but no obvious change in the strength of the Nb steel occurs, which suggests that a small amount of very fine precipitates is formed, likely due to the lower interfacial energy from Mo (Fig. 9) that reduces the energy barrier to nucleation. However, no Nb-rich carbonitrides are seen in the Nb-Mo steel coiled at 900 °C for 100 s using the carbon replica sample preparation method (Fig. 4). This is probably due to the low extraction capability of carbon replica for the particles with diameters < 10 nm.

Preprints (www.preprints.org) | NOT PEER-REVIEWED | Posted: 6 September 2020 doi:10.20944/preprints202009.0150.v1

In recent work by Dorin et al. [13], the shearing to by-passing of the Nb-carbonitrides formed in the austenite was found to occur for a radius of ~ 6 nm. In the present work, the precipitates formed at 900 °C are always larger and we hence assume that they will be by-passed by moving dislocations. As a result, the Friedel's statistical model for Orowan looping [30] can be used to estimate the strength increment from the precipitates:

$$\sigma_p = 0.7MGb\frac{\sqrt{f}}{R} \quad (7)$$

where M is the Taylor factor (~ 3), G is the shear modulus of ferritic matrix (~ 80 GPa [23]), b is the Burgers vector (~ 0.25 nm [23]), f and R are the volume fraction and the radius of precipitates. In this work, the maximum precipitation hardening at each coiling time at 900 °C was calculated using the theoretical volume fraction of Nb carbonitrides under equilibrium calculated by Thermo-Calc software with TCFE 9: Steels/Fe Alloys v9.0 database, 0.0605%, as shown in Table 2.

Table 2. Calculated precipitation hardening (MPa) by Orowan mechanism for the Nb and Nb-Mo steels coiled at 900 °C.

Ageing time	Nb steel	Nb-Mo steel
1000 s	144	171
3000 s	96	140
10,000 s	63	87

The change in yield strength between the as-cast and coiled samples provides a direct measurement of the precipitate hardening for each sample. Figure 10 compares the measured precipitation hardening with the calculated precipitation hardening shown in Table 2. It can be seen that for both alloys the calculated and measured precipitation hardening at 3000 s are very close. For coiling times less than 3000 s the measured strength is lower than the calculated strength, and this is probably because the volume fraction is lower than the maximum. This means that there is still solute available after 1000 s of coiling at 900 °C. After 3000s, the LSW prediction agrees reasonably well with the experimental strength determined from the hardness measurements. For the longest coiling time, the precipitation hardening reduced, which was due to the growth and coarsening of precipitates. Additionally, at 10,000 s, the measured yield strength is slightly lower than the calculated strength, which probably because after a long time coiling the concentration of carbon in solid solution decreases due to precipitation, resulting in lower solid solution strengthening. Furthermore, the coarsening of austenite grains and the formation of allotriomorph ferrite (Figure 2) after a long time coiling may also contribute to the drop in the measured strength.

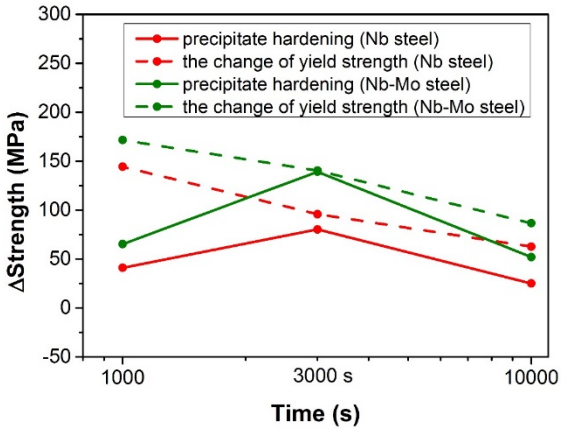

Figure 10 Comparison of the precipitation hardening using the maximum theoretical volume fraction and the change of yield strength for both steels coiled at 900 °C.

5. Conclusions

In the present study, the effect of Mo on the precipitation behaviour in austenite in low-carbon strip-cast steels containing Nb has been investigated. The key conclusions are as follows:

(1) The hardness values of both as-cast steels were similar. During coiling at 900 °C, the hardness of the two steels increased and reached the peak at 3000 s, then decreased after 10000 s coiling. Generally, the Nb-Mo steel had higher hardness than the Nb steel at all coiling times.

(2) The microstructures of both steels coiled at 900 ºC were bainite, only some grain boundary allotriomorph (GBA) were formed in the Nb steels coiled for 10,000 s at 900 °C.

(3) Nb-carbonitrides precipitated in both steels after coiling for 1000 s at 900 °C, and the size of the particles in the Nb-Mo steel was finer than that in the Nb steel. In the Mo-containing steel, Mo also participated in the precipitation, and the concentration of Mo in Nb-rich carbonitrides decreased with increasing particle size and coiling time.

(4) The enrichment of Mo in the Nb-rich carbonitrides reduces the interfacial energy between precipitates and the matrix, which lowers the nucleation energy barrier and the coarsening rate of precipitates.

(5) Strength modelling suggests that precipitation reached maximum volume fraction (0.0605%) after coiling at 900 °C for 3000 s. The precipitates in the Nb-Mo steel imparted an increase in strength up to ~140 MPa, which was much higher than that in the Nb steel, ~ 96 MPa. Further strengthening contributions of the precipitates in both steels decreased after 10,000 s coiling at 900 °C due to the coarsening of the particles.

Acknowledgements: This work was funded by an ARC Discovery Project grant (DP160101540). The authors acknowledge the support of the Deakin Advanced Characterisation Facility. The authors are grateful to Mr David Gray and Dr Adam Taylor for their help with casting the alloys. LJ acknowledges financial support from the Institute Frontier Materials (IFM) through a Student Travel Award, and also the support of Prof. Aimin Bai and Prof. Qilong Yong. Dr. Thomas Dorin is the recipient of an ARC Discovery Early Career Award (DE190100614).

Conflicts of Interest: The authors declare no conflict of interest.

References

[1] S. Hong, K. Kang, C. Park, Strain-induced precipitation of NbC in Nb and Nb–Ti microalloyed HSLA steels, Scripta materialia 46(2) (2002) 163-168.
[2] B. Dutta, C.M. Sellars, Effect of composition and process variables on Nb (C, N) precipitation in niobium microalloyed austenite, Materials Science and Technology 3(3) (1987) 197-206.
[3] A. Le Bon, J. Rofes-Vernis, C. Rossard, Recrystallization and precipitation during hot working of a Nb-bearing HSLA steel, Metal Science 9(1) (1975) 36-40.
[4] W. Lee, S. Hong, C. Park, K. Kim, S. Park, Influence of Mo on precipitation hardening in hot rolled HSLA steels containing Nb, Scripta materialia 43(4) (2000) 319-324.
[5] Y. Xu, M.X. Sun, Y.L. Zhou, Z.Y. Liu, G.D. Wang, Effect of Mo on Nano-Precipitation Behavior and Microscopic Mechanical Characteristics of Ferrite, steel research international 86(9) (2015) 1056-1062.
[6] N. Kamikawa, Y. Abe, G. Miyamoto, Y. Funakawa, T. Furuhara, Tensile behavior of Ti, Mo-added low carbon steels with interphase precipitation, ISIJ international 54(1) (2014) 212-221.
[7] Z. Wang, H. Zhang, C. Guo, W. Liu, Z. Yang, X. Sun, Z. Zhang, F. Jiang, Effect of molybdenum addition on the precipitation of carbides in the austenite matrix of titanium micro-alloyed steels, Journal of materials science 51(10) (2016) 4996-5007.
[8] S. Dhara, R.K.W. Marceau, K. Wood, T. Dorin, I.B. Timokhina, P.D. Hodgson, Precipitation and clustering in a Ti-Mo steel investigated using atom probe tomography and small-angle neutron scattering, Materials Science and Engineering: A 718 (2018) 74-86.

[9] J.H. Jang, Y.U. Heo, C.H. Lee, H.K.D.H. Bhadeshia, D.W. Suh, Interphase precipitation in Ti–Nb and Ti–Nb–Mo bearing steel, Materials Science and Technology 29(3) (2013) 309-313.
[10] C. Chen, H. Yen, F. Kao, W. Li, C. Huang, J. Yang, S. Wang, Precipitation hardening of high-strength low-alloy steels by nanometer-sized carbides, Materials Science and Engineering: A 499(1) (2009) 162-166.
[11] M.G. Akben, B. Bacroix, J.J. Jonas, Effect of vanadium and molybdenum addition on high temperature recovery, recrystallization and precipitation behavior of niobium-based microalloyed steels, Acta Metallurgica 31(1) (1983) 161-174.
[12] J. Cao, Study on the Precipitation of Carbonitride in Nb-Mo-bearing Steel, Dissertation, Kunming University of Science and Technology, 2006.
[13] T. Dorin, K. Wood, A. Taylor, P. Hodgson, N. Stanford, Effect of coiling treatment on microstructural development and precipitate strengthening of a strip cast steel, Acta Materialia 115 (2016) 167-177.
[14] T. Dorin, N. Stanford, A. Taylor, P. Hodgson, Effect of Cooling Rate on Phase Transformations in a High-Strength Low-Alloy Steel Studied from the Liquid Phase, Metallurgical and Materials Transactions A 46(12) (2015) 5561-5571.
[15] L. Strezov, J. Herbertson, Experimental studies of interfacial heat transfer and initial solidification pertinent to strip casting, ISIJ international 38(9) (1998) 959-966.
[16] L. Jiang, R.K.W. Marceau, T. Dorin, P.D. Hodgson, N. Stanford, Effect of molybdenum on phase transformation and microstructural evolution of strip cast steels containing niobium, Journal of Materials Science 54(2) (2019) 1769-1784.
[17] L. Jiang, R.K.W. Marceau, B. Guan, T. Dorin, K. Wood, P.D. Hodgson, N. Stanford, The effect of molybdenum on clustering and precipitation behaviour of strip-cast steels containing niobium, Materialia 8 (2019) 100462.
[18] L. Jiang, R.K.W. Marceau, T. Dorin, K. Wood, P.D. Hodgson, N. Stanford, The effect of molybdenum on interphase precipitation at 700°C in a strip-cast low-carbon niobium steel, Materials Characterization (2020).
[19] W.F. Gale, T.C. Totemeier, Smithells metals reference book, Elsevier2003.
[20] J. Geise, C. Herzig, Lattice and grain boundary diffusion of niobium in iron, Z. Metallkd. 76(9) (1985) 622-626.
[21] P. Alberry, C. Haworth, Interdiffusion of Cr, Mo, and W in iron, Metal Science 8(1) (1974) 407-412.
[22] Q. Yong, Secondary phases in steels, Metallurgical Industry Press, Beijing (2006).
[23] H. Bhadeshia, R. Honeycombe, Steels: microstructure and properties: microstructure and properties, Butterworth-Heinemann2011.
[24] W.C. Leslie, Iron and its dilute substitutional solid solutions, Metallurgical transactions 3(1) (1972) 5-26.
[25] Z.Y. Zhang, Z.D. Li, Q.L. Yong, X.J. Sun, Z.Q. Wang, G.D. Wang, Precipitation behavior of carbide during heating process in Nb and Nb-Mo micro-alloyed steels, Acta Metallurgica Sinica 51(3) (2015) 315-324.
[26] R. Hehemann, Phase transformations, ASM, Metals Park, OH 397 (1970).
[27] I.M. Lifshitz, V.V. Slyozov, The kinetics of precipitation from supersaturated solid solutions, Journal of physics and chemistry of solids 19(1-2) (1961) 35-50.
[28] C. Wagner, Theorie der alterung von niederschlägen durch umlösen (Ostwald-reifung), Berichte der Bunsengesellschaft für physikalische Chemie 65(7-8) (1961) 581-591.
[29] J.T. Busby, M.C. Hash, G.S. Was, The relationship between hardness and yield stress in irradiated austenitic and ferritic steels, Journal of Nuclear Materials 336(2–3) (2005) 267-278.
[30] A. Deschamps, Y. Brechet, Influence of predeformation and ageing of an Al–Zn–Mg alloy—II. Modeling of precipitation kinetics and yield stress, Acta Materialia 47(1) (1998) 293-305.